International Journal of Mechanical, Industrial and Aerospace Sciences
ISSN: 2517-9950
Vol:9, No:7, 2015

On the Numerical and Experimental Analysis of Internal Pressure in Air Bearings

Abdurrahim Dal, Tuncay Karaçay

***Abstract*—**Dynamics of a rotor supported by air bearings is strongly depends on the pressure distribution between the rotor and the bearing. In this study, internal pressure in air bearings is numerical and experimental analyzed for different radial clearances. Firstly the pressure distribution between rotor and bearing is modeled using Reynold's equation and this model is solved numerically. The rotor-bearing system is also modeled in four degree of freedom and it is simulated for different radial clearances. Then, in order to validate numerical results, a test rig is designed and the rotor bearing system is run under the same operational conditions. Pressure signals of left and right bearings are recorded. Internal pressure variations are compared for numerical and experimental results for different radial clearances.

***Keywords*—**Air bearing, internal pressure, Reynold's equation, rotor.

I. Introduction

EXTERNALLY pressurized air bearings are preferred for many industrial application due to their advantages such as low friction, high mechanical endurance and environmental awareness. In air bearing-rotor system, a thin film of air between rotor and bearing surfaces is generated by pressurized air which is supplied by orifices. And this air prevents contact and reduces friction between two surfaces. Dynamics of the rotor is strongly depends on the pressure distribution around the bearing and vice versa. After air makes a thin lubrication film, it exhausts to the atmosphere through the clearance between rotor and bearing with a decreasing pressure. So, it is important to calculate pressure distribution on the supporting surface of air bearing in order to determine the dynamics of the rotor supported.

Researches on the externally pressurized air bearing started with analyzing air flow between rotor and bearing. And then mathematical model of this air flow is obtained with Reynold's equation. In this model, the air flow is represent by a partial differential equation which is depends on geometry of air bearing and operational condition such as rotor speed, supply pressure etc. with the assumptions of ultra-thin film, neglected body force etc. [1]. Over the past decades, many experimentally and theoretically investigations have been focused on improve to this model and obtained the pressure distribution for dynamic analysis of rotor system. Based on the early work, researchers studied about this model with some simplification method such as only axial flow model, infinite length bearing and constant mass flow rate [2]. In 1961, Laub experimentally and theoretically investigated for a semi-cylindrical journal bearing with 9 orifices and a cylindrical journal bearing with 48 orifices each row and he measured pressure between rotor and bearing [3]. He concluded that air flow between rotor and bearing was consist of axial and circumferential flow and improved the air flow model. Powell et al. investigated on a plain cylindrical journal bearing with single row of six feed holes with series of tests and reported that effect of non-axial flow was both to distort the pressure in the clearance space and to reduce the rate of pressure with rotor eccentricity [4]. Then, in 1965, Dudgeon and Lowe modeled air flow between rotor and bearing surfaces by using both axial and circumferential flow and they verified these result by an experimentally study [5]. After these studies, many researchers theoretically and experimentally analyzed effect of air pressure distribution on the dynamics of rotor for different type air bearing and different operational condition [6]-[8]. On the other hand, many studies were investigated on numerical solution of this model for obtaining pressure distribution, in other words, load carrying capacity and dynamic characteristics of air bearing [1]. For obtaining pressure distribution between rotor and bearing, Wang and Chang used Newton method [9], Czolcynski used Alternating Direction Implicit method [10], and Wang et al. used Differential Transform and Finite Difference Hybrid Scheme [11]. In 2004, Park and Kim theoretically and experimentally investigated stability of gas lubricated bearing with a new type slot restrictor, they analyzed pressure distribution and measured only rotor motion at x and y coordinate axes [12]. Chen et al. investigated dynamics characteristic of various geometric designs of externally pressurized air journal bearings for high-speed spindles under different operational conditions. They experimentally evaluated stiffness using the relationship of force and displacement at different feeding parameters. They concluded that the stiffness could be improved with high supply pressure, high L/D ratio and increased orifice diameter [13]. Belforte et al. considered, in an experimental study the effect of discharge coefficient on the pressure distribution. They analyzed pressure distribution with different supply pressure and two types of air feeding systems which were annular orifices and simple orifices with feed pocket [14].

In this study, pressure distribution of externally pressurized air bearing was investigated numerically and experimentally. Air flow between rotor and bearing is modeled using Reynold's equation and solved using Differential Transform & Finite Difference Hybrid numerical solution method. Then an experimental test rig is designed to measure the internal

A. Dal is with the Gazi University, Mechanical Engineering Department, Turkey (e-mail: abdurrahimdal@gazi.edu.tr).

pressure of a point on the control surface. The results show that the numerical simulation values are in good correlation with the experimental data.

II. Mathematical Model and Numerical Analysis

A. Mathematical Modeling and Solution of Air Flow and Bearing-Rotor System

The bearing-rotor system which supported by externally pressurized air bearing, orifices position and coordinate system using for mathematical model are illustrated Fig. 1.

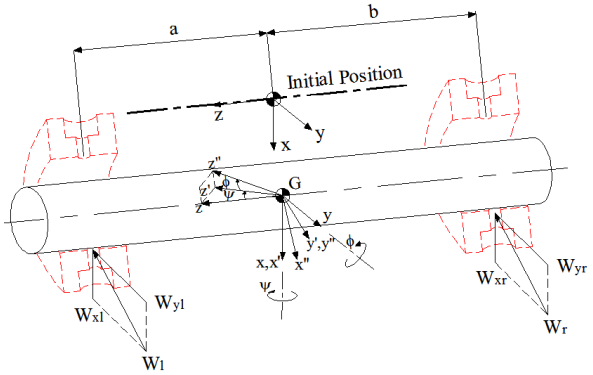

Fig.1 Externally pressurized air bearing rotor system and forces

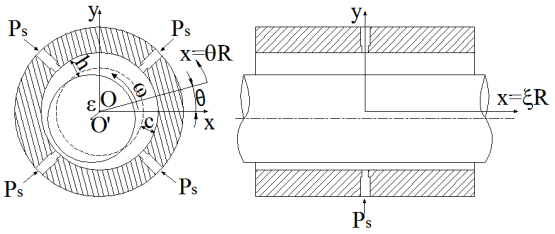

Fig. 2 Schematic view of the externally pressurized air bearing

Equation of motion of the rotor-bearing system could be modeled four degree of freedom Jeffcott rotor model by representing Cartesian coordinate system (see Fig. 1) and given in (1). In this model, it is assumed that rotor doesn't move z-direction; it does only have axial and rotation motion. However, gyroscopic moment effect is included the bearing rotor model. In addition the rotor was assumed unbalanced and it has an eccentricity in order to make a continuous excitation on the rotor. So right hand sides of equations of motion are equal to unbalanced forces and moments.

$$\begin{aligned} m\ddot{x} + W_{x_L} + W_{x_R} - mg &= \delta\omega^2\cos(\omega t) \\ m\ddot{y} + W_{y_L} + W_{y_R} &= \delta\omega^2\sin(\omega t) \\ I_{xx}\ddot{\phi} + aW_{x_L} - bW_{x_R} - I_{zz}\dot{\psi}\omega &= (I_{zz} - I_{xx})\tau\omega^2\cos(\omega t) \\ I_{yy}\ddot{\psi} + aW_{y_L} - bW_{y_R} - I_{zz}\dot{\phi}\omega &= (I_{yy} - I_{xx})\tau\omega^2\sin(\omega t) \end{aligned} \quad (1)$$

In externally pressurized air bearing which is illustrated in Fig. 2, air flow between rotor and bearing surfaces is modeled by using Reynold's equation with dimensionless parameter and it is given in (2),

$$p = P/P_a,\ h = cH,\ x = R\theta,\ z = R\xi,$$

$$U = r\omega,\ \Lambda = \frac{6\mu\omega}{P_a}\left(\frac{R}{c}\right)^2,\ \sigma = \frac{12\mu}{P_a}\left(\frac{R}{c}\right)^2$$

$$\frac{\partial}{\partial\theta}\left[H^3P\frac{\partial P}{\partial\theta}\right] + \frac{\partial}{\partial\xi}\left[H^3P\frac{\partial P}{\partial\xi}\right] + Q = \Lambda\frac{\partial}{\partial\theta}(PH) + \sigma\frac{\partial}{\partial t}(PH) \quad (2)$$

where Pa is atmospheric pressure, H is radial clearance function, θ and ξ cylindrical coordinate systems, and Q is dimensionless mass flow rate which is given in detail [15].

The Reynold's equation is solved using Differential Transform & Finite Difference Hybrid method for pressure distribution between rotors and bearing [16]. The boundary conditions for the solution could be summarized as follows;

1) At the ends of the bearing, pressure value is equal to atmosphere, $P(0,\theta) = P(L,\theta) = P_{atm}$
2) Pressure distribution is a symmetric function for center of bearing length, $P(0 \to L/2,\theta) = P(L/2 \to L,\theta)$
3) Pressure distribution is a continuous at $\xi = 0$
4) Pressure distribution is a periodic function $P(\xi,\theta) = P(\xi,\theta + 2\pi)$,

An iterative procedure, which is based on Runge-Kutta algorithm, issued to obtain motion of the rotor at Cartesian coordinate axes and this is also described in detail in [15]. In this algorithm the external forces are obtained integrating pressure distribution on supporting surfaces of bearings which is obtained by solving Reynold's equation given in (3)

$$\begin{aligned} W_x &= p_a R^2 \int_0^{2\pi}\int_0^{L/R} P(\xi,\theta)\cos\theta\, d\xi d\theta \\ W_y &= p_a R^2 \int_0^{2\pi}\int_0^{L/R} P(\xi,\theta)\sin\theta\, d\xi d\theta \end{aligned} \quad (3)$$

III. Experimental Study

In order to validate numerical solution of the pressure distribution an experimental setup is designed. The externally pressurized air bearing-rotor system used in experimental study is illustrated in Fig. 3. In this system, a rotor is supported by two identical externally pressurized air bearings.

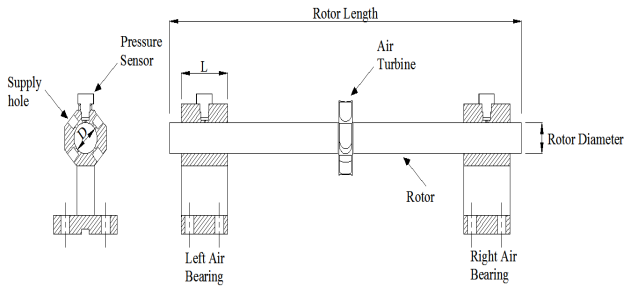

Fig. 3 Major components of externally pressurized air bearing test system

The air bearings have four orifices distributed along the circumference evenly at the middle line of the width. The length to diameter ratio L/D=2. In the test two different bearing set is used with different radial clearances 75 µm and 125 µm. Rotor lengths is 380 mm and rotor diameter is 24.75 mm. The air supplied to the air bearings with conditioned compressor using identical tubing to ensure identical pressure and flow rate at the orifices. And an air turbine system which is located on the rotor is used to give rotation in order to get rid of disturbances caused by mechanical connections and drives such as coupling, driving belt etc.

Schematic representation of the experimental set up with sensors and data acquisition system (DAQ) is given in Fig. 4 and the picture of one of the air bearing is given in Fig. 5. Internal pressures are measured with Kulite Semiconductor HEM-375 pressure transducers and the speed of the rotor is measured with B&K MM-0024 non-contact tachometer. A PC based DAQ system with NI-6052 card is used to measure and store sensor data.

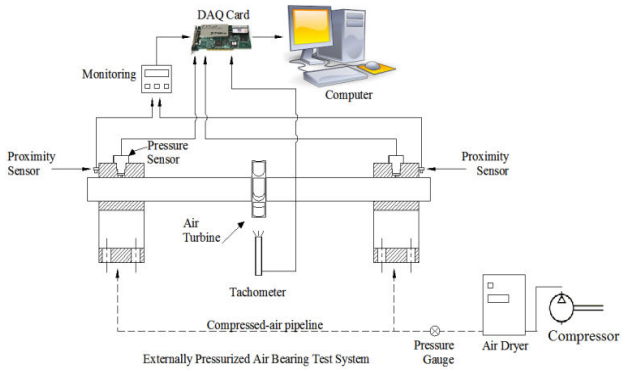

Fig. 4 Schematic view of experimental setup

IV. Results and Discussions

A rotor supported with a pair of air bearing system is analyzed numerically and experimentally to investigate the behavior of internal pressure between the rotor and the bearing clearance. The geometrical dimensions and the air properties used in the simulations are given in Table I. In the simulation and experimental study two different set of air bearing is used with 75µm and 125µm internal clearances.

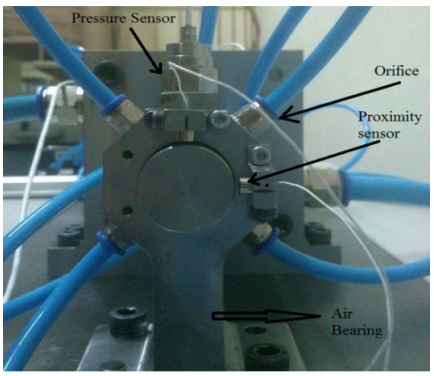

Fig. 5 The air bearing with pressure sensor

TABLE I
Bearings Geometry and Air Properties

Symbol	Quantity	Value
μ	absolute viscosity	18.4×10^{-6}Pa.s
T^0	absolute temperature	298.15 K°
R^0	gas constant	287.6 J/Kg K°
L_R	rotor length	380 mm
D_R	rotor diameter	24.75 mm
d_o	orifices diameter	3 mm
P_s	supply pressure	3 atm
	L/D ratio	2
	number of orifices	4

A. Numerical Results

Pressure distribution between rotor and bearing is obtained using Differential Transform & Finite Difference Hybrid numerical solution method. In this numerical solution, solution grid is 64x96 grids respectively rotor length and circumferential direction, time step is $1x10^{-3}$ and convergence criteria is defined as 10^{-6} between solution steps. Fig. 6 shows three dimensional static pressure distribution of gas bearing under the supply pressure of 3 atm and radial clearance 75 µm. In this simulation the rotor held at the geometrical center of the bearings, i.e. eccentricity is zero, so, pressure distribution is symmetric along the circumferential direction. On the other hand, pressures values at orifices exist are maximum and these values decrease to the ambient (exhaust) pressure levels towards to the end of the bearing.

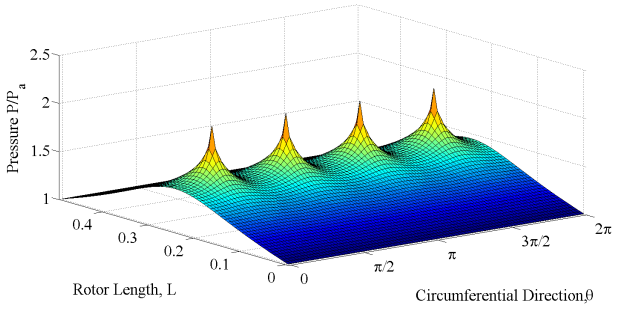

Fig. 6 3D view of pressure distribution at supply pressure 3 atm, eccentricity 0 and radial clearance 75 µm

Pressure values at the air bearing middle cross-section along circumferential direction of gas bearing is given in Fig. 7 for 75 µm and 125µm radial clearances with the supply pressure 3 atm. The pressure values have lower values for higher radial clearance, because the gap volume is higher.

Pressure values between rotor and bearing change with the dynamics of the rotor motion. In this study, equation of motions is simulated with Reynold's equation to obtain internal pressure values between gas bearing and rotor. The supply pressure is set to 3 atm and rotor angular velocity is chosen as 10.000 rpm.

Figs. 8 and 9 show change of pressure value of right and left hand side bearing with respect to time at location of pressure sensor respectively. The radial clearances are 75 µm for both simulations.

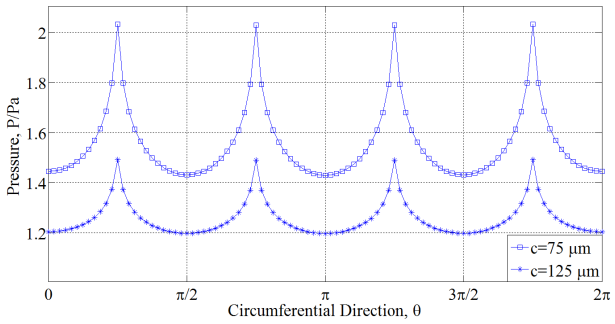

Fig. 7Pressure values at circumferential direction for different radial clearances, supply pressure 3 atm

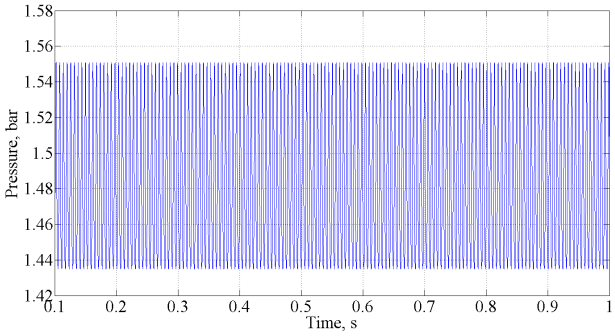

Fig. 8 Pressure values of left bearing vs. time at supply pressure 3 atm and radial clearance 75 µm

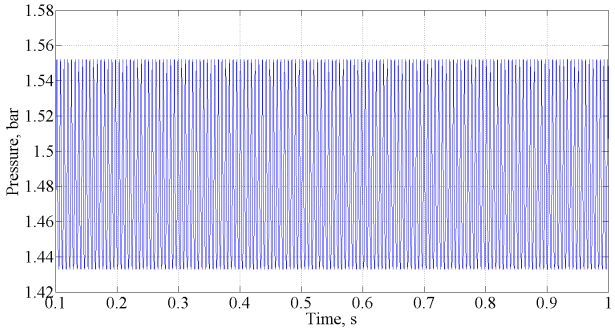

Fig. 9 Pressure values of right bearing vs. time at supply pressure 3 atm and radial clearance 75 µm

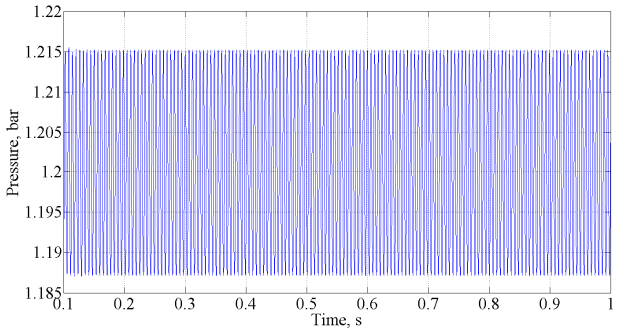

Fig. 10 Pressure values of left bearing vs. time at supply pressure 3 atm and radial clearance 125 µm

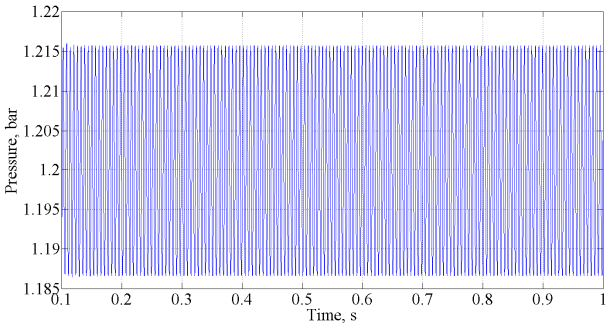

Fig. 11 Pressure values of right bearing vs. time at supply pressure 3 atm and radial clearance 125 µm

Figs. 10 and 11 also show change of pressure value of right and left hand side bearings with respect to time at location of pressure sensor for radial clearance 125 µm.

B. Experimental Results

In order to validate the simulation results a series of test conducted using the same parameter in the simulations. Pressure signal is acquired with pressure transducers and data are analyzed in Matlab environment [17]. The rotor speed is set to 10.000 rpm using non-contact tachometer and air supplied to turbine is cut to eliminate distribution due to rotation excitation. 1 s of data collected for each tests with the sample rate of 10 kHz for each channel. Fig. 12 shows the raw data which is collected from the left hand side bearing pressure transducer. As seen in the figure, raw data has a lot of fluctuation and noise due to high sample rate. Thus, in order to analyze and compare the pressure data, all pressure signals are filtered with a 200 Hz low-pass Butterworth filter which is designed in MATLAB [17].

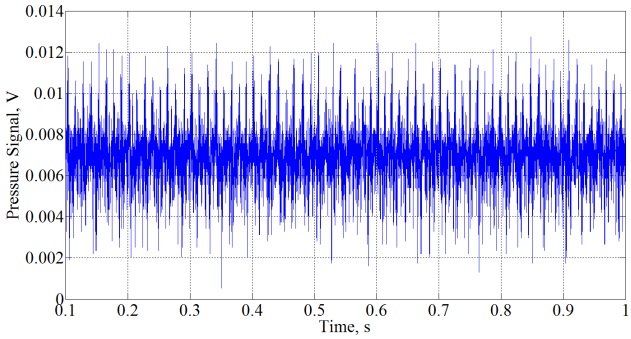

Fig. 12 Pressure data of left bearing vs. time at supply pressure 3 atm and radial clearance 75 µm

Figs. 13 and 14 show variation of internal pressure on the left and right hand side bearing respectively for 75 µm clearance value.

In the air bearing-rotor system, radial clearance between rotor and bearing is an important parameter of the pressure distribution. The variation of internal pressure for 125 µm radial clearances, also is tested with the same operational conditions, and given in Figs. 15 and 16 for the left and right hand side bearing respectively.

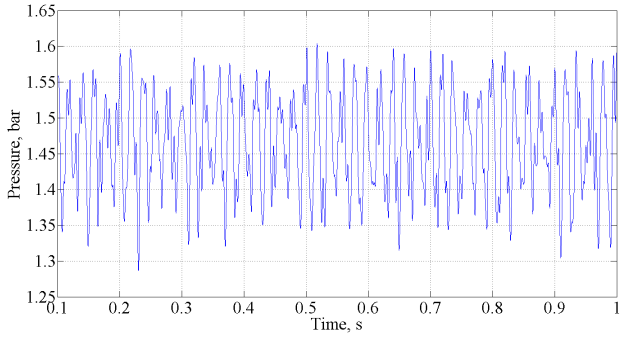

Fig. 13 Filter pressure data with respect to time for left air bearing at supply pressure 3 atm and radial clearance 75 µm

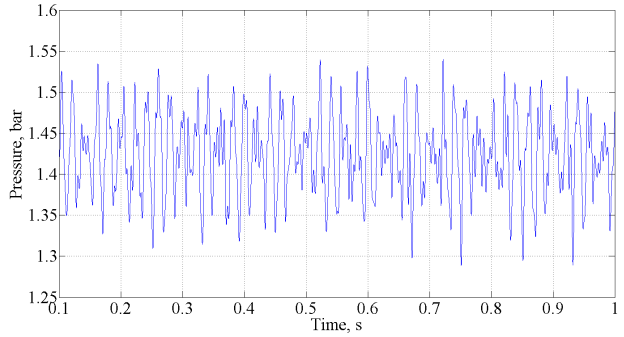

Fig. 14 Filter pressure data with respect to time for right air bearing at supply pressure 3 atm and radial clearance 75 µm

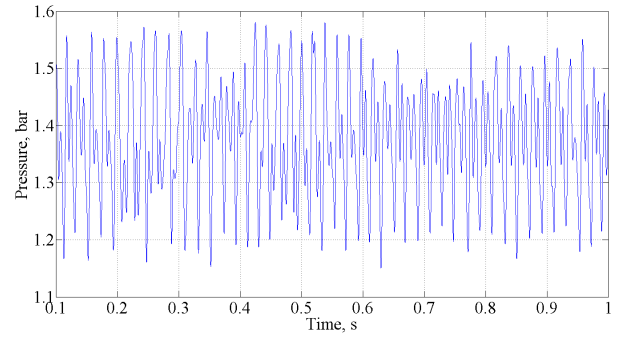

Fig. 15 Filter pressure data with respect to time for left air bearing at supply pressure 3 atm and radial clearance 125 µm

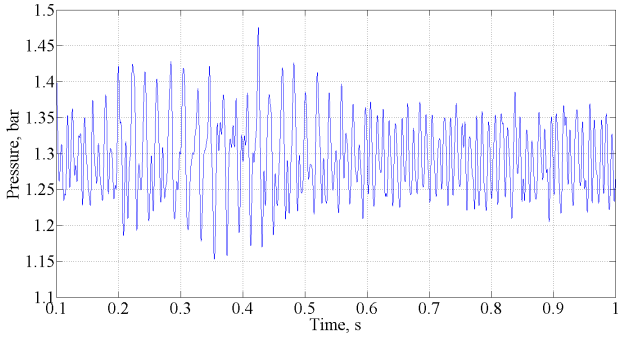

Fig. 16 Filter pressure data with respect to time for right air bearing at supply pressure 3 atm and radial clearance 125 µm

In order to compare numerical and experimental results of pressure distribution, variation limits, mean and RMS values of the internal pressure data are calculated for both support bearings. Tables II and III list the comparison values for 75 µm and 125 µm radial clearances respectively. As seen in the values listed in tables, the difference between experimental and numerical results is quite reasonable. Although the mean or RMS values are almost equal for numerical and experimental results, the variation limits, the minimum and the maximum values of the oscillation, are always higher for experimental results. In the numerical simulation, the pressure distribution is obtained from the solution of Reynold's equation with Differential Transform & Finite Difference Hybrid method. This algorithm has an inherent instability and in order to stabilize solution, a convergences criterion is defined. This criterion controls the variation of pressure values between solution steps. So, it is the reason for close variation around the equilibrium value for pressure distributions.

TABLE II
SCALAR MEASURES OF INTERNAL PRESSURE ACCORDING TO EXPERIMENTAL AND NUMERICAL ANALYSIS FOR LEFT AIR BEARING

Scalar Measures	c=75 µm		c=125 µm	
	Numerical (atm)	Experiment (atm)	Numerical (atm)	Experiment (atm)
Maximum	1.5516	2.6890	1.2309	2.5151
Minimum	1.3915	0.1671	1.1625	0.0372
RMS	1.4819	1.4867	1.2004	1.3975
Mean	1.4815	1.4666	1.2004	1.3754

TABLE III
SCALAR MEASURES OF INTERNAL PRESSURE ACCORDING TO EXPERIMENTAL AND NUMERICAL ANALYSIS FOR RIGHT AIR BEARING

	c=75 µm		c=125 µm	
	Numerical (atm)	Experiment (atm)	Numerical (atm)	Experiment (atm)
Maximum	1.5528	2.2332	1.2315	2.0206
Minimum	1.3961	0.5925	1.1621	0.1671
RMS	1.4804	1.4334	1.2003	1.2943
Mean	1.4808	1.4242	1.2003	1.3043

V. CONCLUSIONS

A rotor supported by two identical air bearing is numerically simulated and experimentally tested to validate pressure distribution in air bearings. The numerical and experimental results show close correlation for the equilibrium state which is calculated as mean value of the pressure variation. However, oscillation amplitude of the numerical values are lower than the experimental values due to convergence criteria defined in the numerical solution of Reynold's equation. The proposed model for the dynamic behavior of the air bearing is satisfactory, but, in order to obtain closer correlation for the numerical model, the values of convergence criteria must be optimized and also different air bearing set with different operational parameters such as supply pressure and rotation speeds needed.

ACKNOWLEDGMENT

This study was supported by the Scientific and Technology

Research Council of Turkey under Grant No 112M847.

REFERENCES

[1] J., Wang, "Design of gas bearing systems for precision application," PhD Thesis, Technische Universiteit, Eindhoven, 1993, pp. 1-35
[2] M., Uneeb, "Theoretical investigation of whirl instability in externally pressurized gas journal bearing," PhD Thesis, Imperial College of Science, Technology and Medicine, London, 1992, pp. 29-92.
[3] J. H., Laub, "Externally Pressurized Gas Bearings," *ASME Journal of Lubrication Technology.,*vol.4 (1), pp. 261, 1961.
[4] J. W. Powell, "Gas behavior and load capacity of hydrodynamic gas journal bearing," *Transactions American Society Lubrication Engineers,* vol. 6, pp. 11, 1963.
[5] E. H. Dudgeon and I., R., G., Lowe, "A theoretical analysis of hydrostatic gas journal bearings," *Mechanical Engineering Report 54,* Canada, 1965, pp. 15-50.
[6] J. S. Ausman, "The fluid dynamic theory of gas lubricated bearing," *Trans. Amer. Soc. Lub. Engrs.,* vol. 79, pp. 1218-1224, 1957
[7] W. J. Lund, "A theoretical analysis of whirl instability and pneumatic hammer for a rigid rotor in pressurized gas journal bearing," *Journal of Lubrication Technology,* vol. 89 pp. 154-165, 1967.
[8] D. Fleming, P. Cunningham, and W, J. Anderson, "Stability analysis for unloaded externally pressurized gas lubricated bearings with journal rotation," *Technical Report TN D-4934,* NASA Levis Research Centre, United States, 1968.
[9] N. Wang and C. Chang, "An application of Newton's method to the lubrication analysis of ari lubricated bearings," *Tribology Transactions,* vol. 42, pp. 419-424, 1998.
[10] K. Czolczynski, "Mathematical model of a gas journal bearing," *Rotordynamics of Gas-Lubricated Journal Bearing System,* Springer, New York, pp. 1-48, 1999.
[11] C. Wang, M. J. Jang, and Y. L. Yeh, "Bifurcation and nonlinear dynamic analysis of a flexible rotor supported by relative short gas journal bearings," *Chaos, Solitons& Fractals,* vol. 32, pp. 566-582, 2007.
[12] J. Park and K. Kim, "Stability analysis and experiments of spindle using new type of slot restricted gas journal bearings," *Tribology International,* vol. 37, pp. 451-462, 2004.
[13] Y. S. Chen, C. C. Chiu, and Y. D. Cheng, "Influences of operational conditions and geometric parameters on the stiffness of aerostatic journal bearings," *Precision Engineering,* vol. 34, pp. 722-734, 2010.
[14] G. Belforte, T. Raparelli, V.Viktorov, and A. Trivella, "Discharge coefficients of orifice-type restrictor for aerostatic bearings," *Tribology International*, vol. 40, pp. 512-521 2007.
[15] A. Dal, and T. Karaçay, "Dynamics of Externally Pressurized Air Bearing with High Values of Clearance," in *ASME 2014 12th Biennial Conference on Engineering Systems Design and Analysis*. Copenhagen, 2014.
[16] T. Karaçay, "Theoretical and experimental investigation of dynamics of rotor supported by externally pressurized air bearings", The Scientific and Technology Research Council of Turkey, Ankara, Technical Report, ARDEB-1001-112M847-2, Oct. 15, 2014 (In Turkish).
[17] MATLAB version 7.0.1, 2004, computer software, The MathWorks Inc., Natick, Massachusetts.